HHS Public Access

Author manuscript

Cell Signal. Author manuscript; available in PMC 2015 April 01.

Published in final edited form as:

Cell Signal. 2015 April ; 27(4): 867–877. doi:10.1016/j.cellsig.2015.01.015.

IQGAP1 regulates actin cytoskeleton organization in podocytes through interaction with nephrin

Yipeng Liu[a,b,1], **Wei Liang**[a,1], **Yingjie Yang**[a], **Yangbin Pan**[a], **Qian Yang**[a], **Xinghua Chen**[a], **Pravin C. Singhal**[c], and **Guohua Ding**[a,*]

[a]Division of Nephrology, Renmin Hospital of Wuhan University, Wuhan, China

[b]Department of Nephrology, Qianfoshan Hospital, Shandong University, Jinan, China

[c]Renal Molecular Research Laboratory, Feinstein Institute for Medical Research, Hofstra North Shore LIJ Medical School, Great Neck, NY, USA

Abstract

Increasing data has shown that the cytoskeletal reorganization of podocytes is involved in the onset of proteinuria and the progression of glomerular disease. Nephrin behaves as a signal sensor of the slit diaphragm to transmit cytoskeletal signals to maintain the unique structure of podocytes. However, the nephrin signaling cascade deserves further study. IQGAP1 is a scaffolding protein with the ability to regulate cytoskeletal organization. It is hypothesized that IQGAP1 contributes to actin reorganization in podocytes through interaction with nephrin. IQGAP1 expression and IQGAP1-nephrin colocalization in glomeruli were progressively decreased and then gradually recovered in line with the development of foot process fusion and proteinuria in puromycin aminonucleoside-injected rats. In cultured human podocytes, puromycin aminonucleoside-induced disruption of F-actin and disorders of migration and spreading were aggravated by IQGAP1 siRNA, and these effects were partially restored by a wild-type IQGAP1 plasmid. Furthermore, the cytoskeletal disorganization stimulated by cytochalasin D in COS7 cells was recovered by cotransfection with wild-type IQGAP1 and nephrin plasmids but was not recovered either by single transfection of the wild-type IQGAP1 plasmid or by cotransfection of mutant IQGAP1 [Δ1443(S → A)] and wild-type nephrin plasmids. Co-immunoprecipitation analysis using lysates of COS7 cells overexpressing nephrin and each derivative-domain molecule of IQGAP1 demonstrated that the poly-proline binding domain and RasGAP domain in the carboxyl terminus of IQGAP1 are the target modules that interact with nephrin. Collectively, these findings showed that activated IQGAP1, as an intracellular partner of nephrin, is involved in actin cytoskeleton organization and functional regulation of podocytes.

Keywords

Actin cytoskeleton; IQ domain GTPase-activating protein 1; Nephrin; Podocyte

*Corresponding author at: Division of Nephrology, Renmin Hospital of Wuhan University, 238 Jiefang Rd, Wuhan, Hubei 430060, China. Tel.: +86 27 88041919 82144; fax: +86 27 88042292. ghxding@gmail.com (G. Ding).

[1]Yipeng Liu and Wei Liang contributed equally to this work.

1. Introduction

Podocytes are terminally differentiated epithelial cells that are essential components of the glomerular filtration barrier, and their injury or depletion plays a pivotal role in the onset of proteinuria and the progression of glomerular diseases [1–6]. Phenotypic alterations in podocytes were detected in a variety of human and experimental glomerular diseases, and foot process (FP) fusion is a unique ultrapathological characteristic of podocyte injury [6–8]. Therefore, discovery of the molecular mechanism of FP fusion could be a crucial step in establishing an effective therapy for podocytopathy.

Previous studies have indicated that cytoskeletal reorganization is the common final pathway of FP fusion [9,10]. The highly ordered parallel contractile actin filament bundles in FP are transformed into disordered, short, branched ones under pathological conditions. Moreover, the elaborate actin cytoskeleton network links the three unique areas of FPs (the apical domain, the slit diaphragm [SD] domain and the basal domain) into structurally and functionally complete units.

A series of molecules are well known to localize to the SD domain of FPs associated with the actin cytoskeleton through scaffold/adaptor proteins, functioning as essential regulators of FP structure and dynamics [11]. Nephrin, the first-described SD protein of podocytes, behaves as a signaling hub to activate several signaling pathways essential for cytoskeletal assembly and cell survival. Collectively, the PI3K-AKT/Rac1, Nck2/N-WASP/Arp2/3, and CD2AP/CapZ/F-actin pathways have been reported to be recruited by nephrin to regulate cytoskeletal dynamics [12–14].

IQ domain GTPase-activating protein 1 (IQGAP1) is a newly discovered scaffolding protein that is also found in the SD region of podocytes [15,16] and contains several functional domains that link multiple signaling molecules, including Rac1/Cdc42, Arp2/3, CLIP-170, E-cadherin, and EGFR. Following interaction with these proteins, IQGAP1 participates in cytoskeletal regulation, ultimately triggering diverse cellular behaviors, such as adhesion, migration, and polarization [17].

Our previous study demonstrated that IQGAP1 had a linear distribution along the capillary loops of glomeruli *in vivo*. Furthermore, IQGAP1 and nephrin colocalized in podocytes [18]. These findings raised our interest regarding whether IQGAP1 contributes to cytoskeletal regulation in podocytes, and whether the function of IQGAP1 in podocytes is realized through interaction with nephrin. In the present study, we used a puromycin aminonucleoside (PAN) nephrosis rat model and PAN-stimulated human podocytes to evaluate the role of IQGAP1 in podocyte cytoskeletal reorganization.

2. Material and methods

2.1. Animals

All experimental procedures were approved by the ethics committee for animal experiments of Wuhan University. Twenty-four male SPF Wistar rats (140 to 160 g) were supplied by the Hubei Research Center of Experimental Animals and raised in a temperature- and humidity-controlled laminar flow room under a 12 h light/12 h dark cycle with free access to

tap water and standard rat chow. The PAN model was established [19] by a single intraperitoneal injection of PAN (15 mg/100 g body weight, Sigma-Aldrich, USA). The 24-h urinary protein was measured on days 0, 4, 7, and 28 after injection. Animals were sacrificed under 10% chloral hydrate anesthesia on day 0, 4, 7, or 28. Kidneys were perfused with the phosphatase inhibitor vanadate before harvest. Part of the kidney was used for the isolation of glomeruli. The cortex of the rest of the kidney was separated and fixed in 4% phosphate-buffered paraformaldehyde, glutaraldehyde, or tissue-freezing medium for renal pathological and immunofluorescence analysis.

Glomeruli were isolated by the differential sieving method [20,21]. The renal cortex was separated and successively passed through three stainless steel sieves with pore sizes of 177 μm (80 mesh), 125 μm (120 mesh), and 74 μm (200 mesh). D-Hank's buffer containing vanadate was used for the continuous rinsing of debris. Glomeruli collected from the last sieve were harvested and used for Western blotting analysis.

Transmission electron microscopy was used to evaluate the ultra-structural changes of podocytes. Briefly, 2.5% glutaraldehyde-fixed 1-mm^3 blocks of renal cortices were postfixed with 1% osmic acid, dehydrated in graded ethanol, embedded in EPON, sectioned, stained with uranyl acetate and lead citrate, and then observed and recorded with a Hitachi H-600 transmission electron microscope (Hitachi, Japan). The mean FP width was defined as the total length of the glomerular basement membrane (GBM) divided by the total number of FPs. The FP fusion rate was presented as the length of FP fusion divided by the total length of the GBM.

2.2. Cell culture

Conditionally immortalized human podocytes were provided by Dr. Moin A. Saleem (Academic Renal Unit, Southmead Hospital, Bristol, UK) and cultured in RPMI 1640 medium (HyClone, USA) containing 10% fetal bovine serum (Gibco, USA), 1× penicillin–streptomycin, and 1 mM L-glutamine in a 5% CO_2 incubator. During the proliferation phase, 1× insulin, transferrin, and selenium (ITS) (Invitrogen, USA) was added to the medium, and the cells were subcultured at 33 °C. These cells were cultured in a 37 °C incubator with ITS-free medium for 7 days to induce differentiation.

COS7 cells were purchased from the Cell Resource Center of Shanghai Institutes for Biological Sciences, Chinese Academy of Sciences, and cultured in a 37 °C incubator in DMEM (Corning, USA) containing 10% fetal bovine serum (Gibco, USA). G418 (Sigma-Aldrich, USA) was used to select stably transfected nephrin cell lines (NCOS7). When the cells had grown to approximately 60% confluence, 20 μg/mL cytochalasin D (CyD, Enzo Life Sciences, Switzerland) was added to the medium for 30 min to depolymerize the actin cytoskeleton [22].

2.3. Plasmid construction and transfection

The full-length expression plasmids of nephrin (pcDNA3.1-NPHS1) and IQGAP1 (pCAN-myc-IQGAP1) were kindly provided by Dr. Lawrence B Holzman (University of Michigan Medical School, MI, USA) and Dr. Jon Erickson (Cornell University, NY, USA), respectively. The Δ1443(S → A) IQGAP1 mutant plasmid was constructed by mutating the

serine to alanine to inhibit IQGAP1 phosphorylation. The pEGFP-C1 eukaryotic expression vector was purchased from Clontech (USA) and reformed to carry a Myc tag (pEGFP-C1-Myc). The Myc primers used in PCR amplification were as follows: sense: 5′-TCTGAAGAGGATCTGTCCGGACTCAGATCTC-3′ and anti-sense: 5′-CAGATCCTCTTCAGAGATGAGTTTCTGCTCCTTGTACAGCTCGT CC-3′. The calponin homology domain (CHD), the IQGAP-specific repeat motif (IR), the poly-proline binding domain (WW), the calmodulin-binding motif (IQ), the RasGTPase-activating protein-related domain (GRD), and the RasGAP domain in the carboxyl terminus (RGCT) of IQGAP1 were then subcloned into pEGFP-C1-Myc. Detailed information for the plasmids is shown in Table 1.

For plasmid transfection, 6×10^5 cells were seeded into a 100-mm dish and incubated with transfection complexes containing 5 μg relevant plasmid and 15 μL X-tremeGENE HP DNA Transfection Reagent (Roche, Germany) under growth conditions for 72 h.

2.4. Transfection of IQGAP1 siRNA

Transfection of podocytes with IQGAP1 siRNA was performed according to the HiPerFect Transfection Reagent Handbook (QIAGEN, Germany). Briefly, 3×10^6 cells were seeded into a 100-mm dish and incubated with transfection complexes containing 5 nM IQGAP1 siRNA (or scrambled siRNA) and 40 μL HiPerFect transfection reagent under growth conditions for 48 h.

2.5. Immunofluorescence assay

The frozen kidney sections (5-μm thick) were blocked with 5% BSA for 30 min at 37 °C, and cell-climbing films were fixed with 4% paraformaldehyde for 30 min at 4 °C. The samples were then incubated with a mixture of nephrin guinea pig primary polyclonal antibody (pAb, 1:50; PROGEN Biotechnik, Germany) and IQGAP1 rabbit primary pAb (1:50; Santa Cruz, USA) overnight at 4 °C, as well as with a secondary antibody mixture of FITC-conjugated goat anti-guinea pig IgG (1:100, Santa Cruz, USA) and TRITC-conjugated goat anti-rabbit IgG (1:100, Thermo scientific, USA) at 37 °C for 90 min in darkness. The samples were examined using a confocal fluorescence microscope (FV-500, Olympus, Japan).

2.6. Real-time PCR

Total RNA was extracted from podocytes using TRIzol reagent (Invitrogen, USA). The concentration of collected RNA was measured by spectrophotometry. After the cDNA was synthesized, the study was performed with the real-time fluorescent quantitative PCR machine (Illumina Eco, USA). The specificity of real-time PCR was detected by melting-curve analysis. β-actin was used as internal standard. The primers used in this study were as follows: IQGAP1, sense: 5′-GGGG AAACGTACCAGAGTGA-3′ and anti-sense: 5′-TCTCGAGAAAGCTGCACA GA-3′; β-actin, sense: 5′-CACGATGGAGGGGCCGGACTCATC-3′ and anti-sense: 5′-TAAAGACCTCTATGCCAACACAGT-3′.

2.7. Western blotting

The protein concentration was measured using a BCA protein assay (Thermo Scientific, USA). Equal amounts of boiled protein in loading buffer were separated using NuPAGE 10% Bis-Tris SDS-PAGE (Life Technologies, USA) and then electrophoretically transferred to polyvinylidene fluoride membranes (Millipore, USA). The membranes were incubated with primary antibodies (nephrin rabbit pAb, 1:200, Abcam, UK; p-nephrin rabbit monoclonal antibody [mAb], 1:10,000, Abcam, UK; IQGAP1 rabbit pAb, 1:200, Santa Cruz, USA; p-serine [p-Ser] mouse mAb, 1:300, Millipore, USA; Myc mouse mAb, 1:2000, California Bioscience, USA; β-actin mouse mAb, 1:1000, Santa Cruz, USA) overnight at 4 °C, followed by incubation with a secondary antibody (LICOR, Lincoln, NE, USA), and the membranes were then analyzed using the ODESSEY infrared imaging system (LICOR, Lincoln, NE, USA). The integrated optical density for each band was calculated using a Gel-Pro Analyzer, version 4.5.

2.8. Co-immunoprecipitation

Co-immunoprecipitation experiments were conducted according to the manufacturer's instructions (P2012, Beyotime, China). The total protein of the cultured podocytes or COS7 cells was extracted using lysis buffer (1.0% Triton X-100, 150 mM NaCl, 5 mM EDTA, 1 mM PMSF, 20 mM Tris, pH 7.5) that contained a protease inhibitor cocktail (P8340, Sigma-Aldrich, USA). The samples were centrifuged at 13,000 *g* for 5 min at 4 °C. Nephrin rabbit pAb (2 μg/500 μg total protein; Santa Cruz, USA) or IQGAP1 rabbit pAb (2 μg/500 μg total protein, Santa Cruz, USA) was added to the supernatant and rotated overnight at 4 °C. Then, the mixture was loaded with protein A + G agarose and incubated for 3 h at 4 °C. The centrifuged sediment was saved and mixed with 1× LDS sample buffer. After boiling at 70 °C for 10 min, the samples were analyzed by Western blotting.

2.9. Staining of the actin cytoskeleton

The cells were fixed with 4% paraformaldehyde at 4 °C for 30 min, washed with ice-cold phosphate-buffered saline 3 times for 5 min, and stained with 2.5 μg/mL FITC-phalloidin (Sigma-Aldrich, USA) for 1 h at room temperature. Finally, the samples were viewed using a confocal fluorescence microscope (FV-500, Olympus, Japan), and the cortical F-actin score (CFS) was assessed as previously described [23] to quantify the degree of cytoskeletal reorganization.

Concretely, the cytoskeletal reorganization for each cell was scored on a scale ranging from 0 to 3 based on the degree of cortical F-actin ring formation (score = 0, no cortical F-actin, normal stress fibers; score = 1, cortical F-actin deposits below ½ of the cell border; score = 2, cortical F-actin deposits exceeding ½ of the cell border; score = 3, complete cortical ring formation and/or total absence of central stress fibers).

2.10. Cell migration and spreading assays

For the migration assay, 2 wounds per well were made with a sterile pipet tip after the cells had grown to complete confluence in a 6-well plate. Pictures were taken just before (0 h)

and 6 h after scraping with an inverted phase-contrast microscope. To estimate cell migration, the number of cells crossing the 1-mm wound border was calculated.

For the spreading assay, cells (2×10^5) were seeded into a 6-well plate after being digested by pancreatin. The morphology of podocytes was observed after 6 h under an inverted phase-contrast microscope. Spread cells had extended processes, whereas unspread cells were round. The percentage of spreading podocytes was defined as the number of spread cells divided by the total number of cells.

2.11. Statistical analysis

The values are presented as the means ± SDs, and the statistical analysis was performed using SPSS ver. 17.0. A statistical comparison of the groups was conducted using one-way ANOVA, and the LSD test was used for multiple comparisons. $P < 0.05$ was considered statistically significant.

3. Results

3.1. The expression and distribution of IQGAP1 in the glomeruli of rats with PAN nephrosis

We established a rat model of PAN nephrosis to investigate the pathogenesis of FP fusion and proteinuria. The PAS staining and proteinuria data (Fig. 1A, B and C) showed that protein cast was present in the renal tubular lumen on day 4, and heavier proteinuria was found on day 7. However, the proteinuria recovered on day 28 after the injection of PAN. Ultrastructure analysis of podocyte (Fig. 1D) indicated that the mean FP width and FP fusion rate developed on the same time-course as that of proteinuria.

Next, we performed Western blotting and immunolabeling to detect the expression and distribution of IQGAP1 in glomeruli. As shown in Fig. 1E and F, the expression level of IQGAP1 was dramatically decreased on days 4 and 7 and then returned to the control level on day 28 after PAN injection. Interestingly, the IQGAP1-nephrin colocalization in glomeruli were progressively suppressed and gradually recovered in line with the development of FP fusion and proteinuria in PAN-injected rats.

3.2. Effect of PAN on the expression of IQGAP1 in vitro

Previous studies have indicated that IQGAP1 is expressed in the SD of podocytes, but its exact role in podocytopathy is still elusive. *In vitro*, we exposed differentiated human podocytes to PAN to investigate the possible role of IQGAP1 in podocyte injury. As shown in Fig. 2, PAN exposure induced decreased IQGAP1 mRNA and protein expression in a dose- and time-dependent manner.

3.3. Effects of PAN on IQGAP1 phosphorylation and the interaction between IQGAP1 and nephrin

The colocalization pattern of IQGAP1 and nephrin in the glomeruli of rats with PAN nephrosis impelled us to explore the functional role of the interaction between IQGAP1 and nephrin in podocytes. As shown in Fig. 3A and B, double immunolabeling and co-immunoprecipitation analysis indicated that PAN exposure significantly decreased the

interaction between IQGAP1 and nephrin in cultured podocytes. Moreover, the serine phosphorylation of IQGAP1 was also obviously suppressed by PAN treatment (Fig. 3C).

3.4. Role of IQGAP1 in cytoskeletal regulation

We used IQGAP1 siRNA and plasmids to regulate the endogenous expression of IQGAP1 in human podocytes to evaluate its role in the signaling pathway of cytoskeletal reorganization. After transfecting human podocytes with IQGAP1 siRNA or plasmids, the expression of IQGAP1 was examined by Western blotting analysis. As shown in Fig. 4A and B, IQGAP1 siRNA significantly decreased IQGAP1 expression whereas the IQGAP1 plasmid dramatically increased its expression ($P < 0.05$), indicating the successful interference of IQGAP1 expression. However, the expression of nephrin and phosphorylated nephrin were not affected in IQGAP1 siRNA- or plasmid-transfected cells.

Interestingly, the alteration of IQGAP1 expression influenced the interaction between IQGAP1 and nephrin. The downtrend of IQGAP1 co-immunoprecipitated with nephrin after PAN stimulation was aggravated by IQGAP1 siRNA transfection and partially restored by wild-type IQGAP1 plasmid transfection (Fig. 4C).

Furthermore, fluorescent analysis of the actin cytoskeleton demonstrated that stress fibers in normal cells were disorganized by PAN treatment, and a peripheral actin rim and scattered actin fragments were found in PAN-treated cells. Moreover, PAN-induced F-actin disruption was aggravated by knocking down endogenous IQGAP1 and partly rescued by overexpressing IQGAP1 (Fig. 4D).

3.5. Roles of IQGAP1 in podocyte function

The crucial role of cytoskeletal organization in podocyte function has been widely recognized, so we further evaluated the involvement of IQGAP1 in various podocyte functions, such as cell migration and spreading. As shown in Fig. 5, PAN stimulation apparently provoked podocyte migration but inhibited podocyte spreading ($P < 0.05$). Additionally, IQGAP1 siRNA further significantly enhanced cell migration, whereas IQGAP1 overexpression dramatically weakened migration to nearly normal levels. Conversely, the PAN-induced inhibition of cell spreading was progressively worsened by transfection with IQGAP1 siRNA and partially recovered by transfection with the wild-type IQGAP1 plasmid.

3.6. Involvement of the nephrin–IQGAP1 interaction and IQGAP1 phosphorylation in cytoskeletal regulation

To investigate the involvement of the nephrin–IQGAP1 interaction and IQGAP1 phosphorylation in cytoskeletal regulation, we established an NCOS7 cell line with nephrin overexpression and then transfected these cells with wild-type and Δ1443(S → A) mutant IQGAP1 plasmids, respectively. As shown in Fig. 6A, the transfections were successful. Moreover, the stress fibers in COS7 and NCOS7 cells were obviously disrupted by CyD (a cytoskeleton depolymerizing agent). Single transfection with either the wild-type or Δ1443(S → A) mutant IQGAP1 plasmid did not rescue the stress fibers of the F-actin cytoskeleton in CyD–treated COS7 cells. However, in NCOS7 cells, transfection with the

wild-type IQGAP1 plasmid dramatically restored CyD-induced cytoskeletal disorganization, which was not found in Δ1443(S → A) mutant IQGAP1 plasmid-transfected NCOS7 cells (Fig. 6B).

3.7. The WW and RGCT domains of IQGAP1 are the nephrin binding sites

Next, we proceeded to identify the domains of IQGAP1 that are responsible for binding to nephrin. Co-immunoprecipitation analysis demonstrated that the WW and RGCT domains are necessary for the binding of IQGAP1 to nephrin (Fig. 7).

4. Discussion

Podocyte FP fusion and proteinuria are common symptoms of a series of glomerular diseases, such as minimal change nephropathy (MCD) [24], membranous nephropathy [25], focal segmental glomerulosclerosis [26], and diabetic nephropathy [27]. FP fusion is the characteristic feature of podocyte injury. In the present study, we established a PAN nephrosis rat model that mimics the podocyte injury of human MCD [28]. Apart from the classical features of urinary protein excretion and FP morphology, concomitant alterations of IQGAP1 expression and its colocalization with nephrin were also found in PAN-injected rats, suggesting that the nephrin–IQGAP1 signaling cascade might participate in the regulation of FP function.

IQGAP1 is the best-studied member of the IQGAP family, which comprises IQGAP1, IQGAP2, and IQGAP3. IQGAP1 is evolutionarily conserved and expressed in numerous species [29]. As a scaffolding protein, IQGAP1 contains several domains that are essential for binding to target proteins: the CHD domain in the N-terminus, followed by the IR domain, the WW domain, the IQ domain, the GRD domain, and the RGCT domain. Through interactions with numerous membrane proteins, such as E-cadherin, CXCR2, EGFR, and NGFR, IQGAP1 transmits extracellular stimuli to the intracellular cytoskeletal network [17].

Accumulating evidence has demonstrated that cytoskeletal reorganization is the common final pathway of FP fusion. Our results showed that PAN-induced F-actin disruption was exacerbated by IQGAP1 downregulation and partially recovered by IQGAP1 upregulation, which suggests that IQGAP1 is essential in the regulation of cytoskeletal organization. FP fusion is a migratory event of podocytes [30]. IQGAP1 downregulation promoted podocyte migration, which was weakened by IQGAP1 overexpression. Meanwhile, IQGAP1 is also able to modulate the spreading activity of podocytes. All of the functional experiments suggest that IQGAP1 is crucial to maintain the relatively quiescent and digitate spreading phenotype of podocytes. Rigothier et al. [16] similarly reported that IQGAP1 is involved in podocyte barrier properties through interactions with cytoskeletal proteins in human podocytes. However, the role of IQGAP1 in migration in Rigothier's study contradicts the present data. Differences in the stimulating factor and the intensity, as well as complicated compensation mechanisms in the IQGAP family, might explain the discrepancy among studies.

Nephrin is an essential SD protein in podocytes that acts as a structural protein to maintain the integrity of the glomerular filtration barrier and also as a signaling hub to transmit extracellular stimuli into the cytoplasm and to maintain podocyte cell viability and mobility [31]. In PAN-stimulated podocytes, actin cytoskeletal remodeling is accompanied by the altered colocalization of IQGAP1 and nephrin. Furthermore, the verification test using COS7 cells showed that IQGAP1 transfection ameliorated CyD-induced cytoskeletal disorganization only with the coexistence of nephrin, suggesting that IQGAP1 exerts its cytoskeletal regulatory function through interaction with nephrin. Moreover, a defect of IQGAP1 was able to disturb its interaction with nephrin and induce cytoskeletal disorganization, indicating that IQGAP1 builds a bridge between the nephrin signaling hub and the cytoskeleton network in podocytes.

Additionally, the diverse functions of IQGAP1 are regulated by its phosphorylation [32]. This protein is inactive when its two C-terminal domains, GRD and RGCT, associate with each other, resulting in intramolecular inhibition. PKC-induced Ser^{1443} phosphorylation can relieve this intramolecular masking and expose the membrane protein and F-actin binding sites [33]. Upon mutating the serine (1443) to alanine to inhibit IQGAP1 phosphorylation, mutant IQGAP1 plasmid transfection could not alleviate CyD-stimulated cytoskeletal disorganization in NCOS7 cells, suggesting that the phosphorylation state of IQGAP1 is crucial for its function in cytoskeletal regulation.

A previous study [34] reported that the C-terminal half of the nephrin intracellular domain (amino acids 1167–1256) is responsible for IQGAP1 binding. The present research consummated the above study and found that the WW and RGCT domains are the specific binding sites of IQGAP1 to nephrin. These two domains are crucial for IQGAP1 to bind several signaling proteins, such as ERK2, CLIP-170,β-catenin and APC, contributing to the diversity of IQGAP1 functions in cellular pathophysiology.

In conclusion, the current study shows, for the first time, that phosphorylated IQGAP1 interacts with nephrin through its WW and RGCT domains, exerts its regulatory function in actin cytoskeleton organization, and ultimately contributes to regulating FP morphology and podocyte function (Fig. 8). Therefore, the scaffolding protein IQGAP1 might be a new effective therapeutic target for podocytopathy.

Acknowledgments

This work wass upported by grants from the National Science Foundation of China (81100478 to W. Liang and 81270762 to G. Ding) and the Fundamental Research Funds for the Central Universities (2012302020204 to Y. Liu).

References

1. Arif E, Rathore YS, Kumari B, Ashish F, Wong HN, Holzman LB, Nihalani D. J Biol Chem. 2014; 289(14):9502–9518. [PubMed: 24554715]
2. Brosius FC, Coward RJ. Adv Chron Kidney Dis. 2014; 21(3):304–310.
3. Daehn I, Casalena G, Zhang T, Shi S, Fenninger F, Barasch N, Yu L, D'Agati V, Schlondorff D, Kriz W, Haraldsson B, Bottinger EP. J Clin Invest. 2014; 124(4):1608–1621. [PubMed: 24590287]
4. Nangaku M, Shankland SJ, Couser WG. J Am Soc Nephrol. 2005; 16(5):1195–1204. [PubMed: 15800119]

5. Mathieson PW. Semin Immunopathol. 2007; 29(4):415–426. [PubMed: 17955243]
6. Mundel P, Reiser J. Kidney Int. 2010; 77(7):571–580. [PubMed: 19924101]
7. Sedor JR, Madhavan SM, Kim JH, Konieczkowski M. Trans Am Clin Climatol Assoc. 2011; 122:184–197. [PubMed: 21686224]
8. Jeruschke S, Buscher AK, Oh J, Saleem MA, Hoyer PF, Weber S, Nalbant P. PLoS One. 2013; 8(2):e55980. [PubMed: 23418489]
9. Schell C, Baumhakl L, Salou S, Conzelmann AC, Meyer C, Helmstadter M, Wrede C, Grahammer F, Eimer S, Kerjaschki D, Walz G, Snapper S, Huber TB. J Am Soc Nephrol. 2013; 24(5):713–721. [PubMed: 23471198]
10. Wang L, Ellis MJ, Gomez JA, Eisner W, Fennell W, Howell DN, Ruiz P, Fields TA, Spurney RF. Kidney Int. 2012; 81(11):1075–1085. [PubMed: 22278020]
11. Greka A, Mundel P. Annu Rev Physiol. 2012; 74:299–323. [PubMed: 22054238]
12. Faul C, Asanuma K, Yanagida-Asanuma E, Kim K, Mundel P. Trends Cell Biol. 2007; 17(9):428–437. [PubMed: 17804239]
13. Patrakka J, Tryggvason K. Trends Mol Med. 2007; 13(9):396–403. [PubMed: 17766183]
14. Zhu J, Sun N, Aoudjit L, Li H, Kawachi H, Lemay S, Takano T. Kidney Int. 2008; 73(5):556–566. [PubMed: 18033240]
15. Lehtonen S, Ryan JJ, Kudlicka K, Iino N, Zhou H, Farquhar MG. Proc Natl Acad Sci U S A. 2005; 102(28):9814–9819. [PubMed: 15994232]
16. Rigothier C, Auguste P, Welsh GI, Lepreux S, Deminiere C, Mathieson PW, Saleem MA, Ripoche J, Combe C. PLoS One. 2012; 7(5):e37695. [PubMed: 22662192]
17. White CD, Erdemir HH, Sacks DB. Cell Signal. 2012; 24(4):826–834. [PubMed: 22182509]
18. Liu Y, Liang W, Yang Q, Ren Z, Chen X, Zha D, Singhal PC, Ding G. Am J Nephrol. 2013; 38(5): 430–444. [PubMed: 24247724]
19. Uchida K, Suzuki K, Iwamoto M, Kawachi H, Ohno M, Horita S, Nitta K. Kidney Int. 2008; 73(8): 926–932. [PubMed: 18256598]
20. Burlington H, Cronkite EP. Proc Soc Exp Biol Med. 1973; 142(1):143–149. [PubMed: 4118960]
21. Kreisberg JI, Wilson PD. J Electron Microsc Technol. 1988; 9(3):235–263.
22. Schliwa M. J Cell Biol. 1982; 92(1):79–91. [PubMed: 7199055]
23. Hsu HH, Hoffmann S, Endlich N, Velic A, Schwab A, Weide T, Schlatter E, Pavenstadt H. J Mol Med (Berl). 2008; 86(12):1379–1394. [PubMed: 18773185]
24. Chugh SS, Clement LC, Mace C. Am J Kidney Dis. 2012; 59(2):284–292. [PubMed: 21974967]
25. Arabi Z, Avicenna. J Med. 2012; 2(3):60–64.
26. Schell C, Huber TB. Nephrol Dial Transplant. 2012; 27(9):3406–3412. [PubMed: 22767631]
27. Tufro A, Veron D. Semin Nephrol. 2012; 32(4):385–393. [PubMed: 22958493]
28. Furness PN, Harris K. Int J Exp Pathol. 1994; 75(1):9–22. [PubMed: 8142275]
29. Briggs MW, Sacks DB. EMBO Rep. 2003; 4(6):571–574. [PubMed: 12776176]
30. Reiser J, Oh J, Shirato I, Asanuma K, Hug A, Mundel TM, Honey K, Ishidoh K, Kominami E, Kreidberg JA, Tomino Y, Mundel P. J Biol Chem. 2004; 279(33):34827–34832. [PubMed: 15197181]
31. Li M, Armelloni S, Edefonti A, Messa P, Rastaldi MP. Nephrol Dial Transplant. 2013; 28(4):767–770. [PubMed: 23139403]
32. Heil A, Nazmi AR, Koltzscher M, Poeter M, Austermann J, Assard N, Baudier J, Kaibuchi K, Gerke V. J Biol Chem. 2011; 286(9):7227–7238. [PubMed: 21177863]
33. Grohmanova K, Schlaepfer D, Hess D, Gutierrez P, Beck M, Kroschewski R. J Biol Chem. 2004; 279(47):48495–48504. [PubMed: 15355962]
34. Liu XL, Kilpelainen P, Hellman U, Sun Y, Wartiovaara J, Morgunova E, Pikkarainen T, Yan K, Jonsson AP, Tryggvason K. FEBS J. 2005; 272(1):228–243. [PubMed: 15634346]

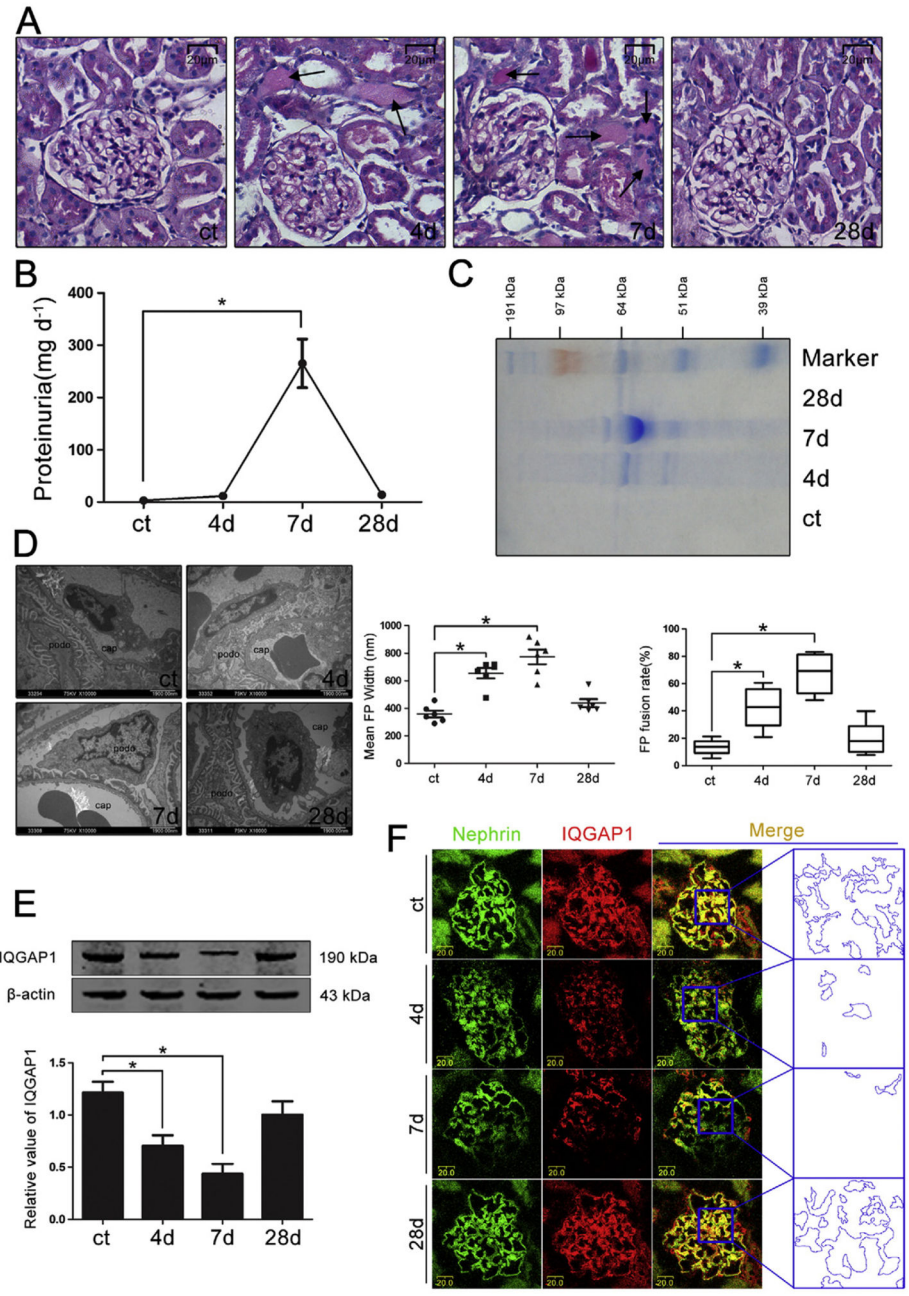

Fig. 1.

The expression and distribution of IQGAP1 in glomeruli during PAN nephrosis. (A) Representative microscopy images of renal pathological changes in various groups (PAS staining, original magnification ×200). Scale bar = 20 μm. The black arrows indicate protein cast in the renal tubular lumen. (B) Quantitative analysis of urinary protein excretion in various groups (n = 6). (C) Coomassie brilliant blue staining of urinary protein in various groups. (D) Representative transmission electron microscopy images of glomerular capillary walls (original magnification ×10,000) and quantitative analysis of the FP width and FP fusion rate (n = 6). Scale bar = 1900 nm. Podo, podocyte. Cap, capillary lumen. (E) Western

blotting analysis of glomerular IQGAP1 in various groups ($n = 6$). (F) Double immunolabeling of nephrin and IQGAP1 in glomeruli (original magnification ×400). The colocalization area of nephrin and IQGAP1 indicated by the blue dotted line is an enlarged view of the boxed region. Scale bar = 20 μm. *$p < 0.05$ relative to control.

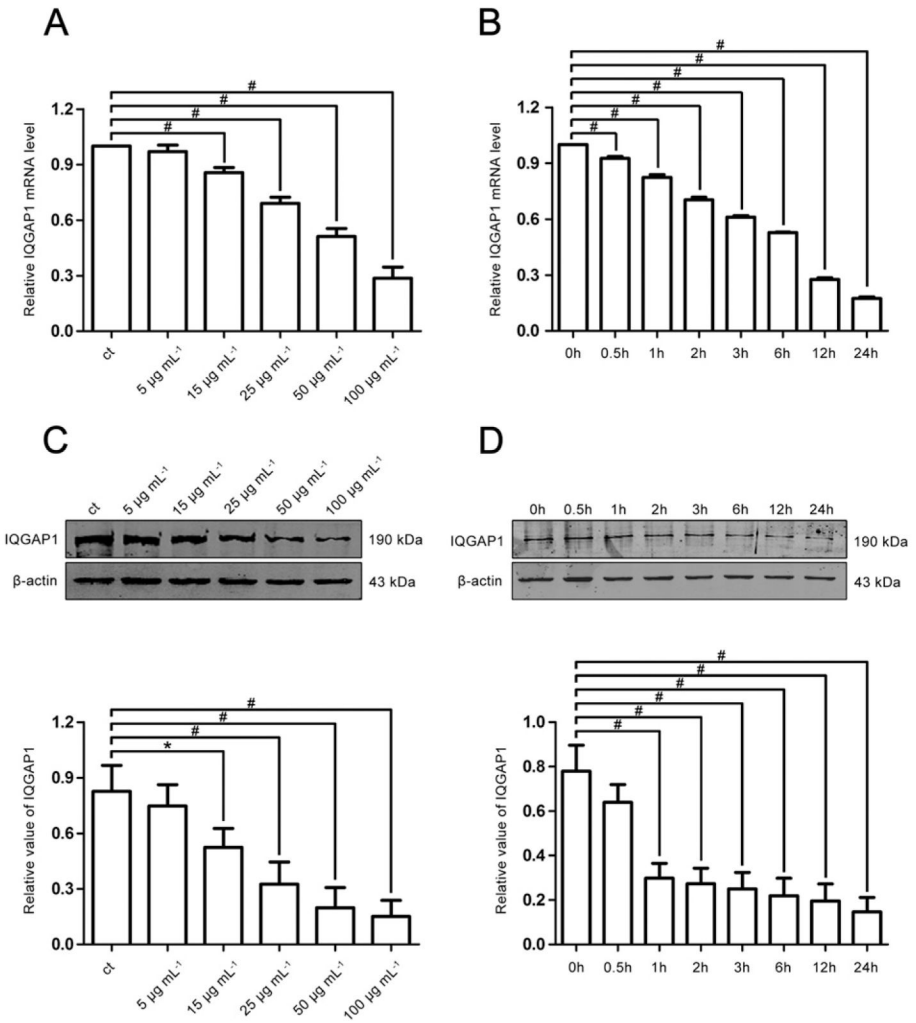

Fig. 2.

The expression of IQGAP1 in podocytes stimulated by PAN. (A) (B) Real-time PCR analysis of IQGAP1 expression in cultured podocytes stimulated by various concentrations of PAN for 6 h or by 50 μg mL^{-1} PAN for 0–24 h ($n = 3$). (C) (D) Western blotting analysis of IQGAP1 expression in cultured podocytes treated with PAN ($n = 3$). *$p < 0.05$, #$p < 0.01$ relative to control.

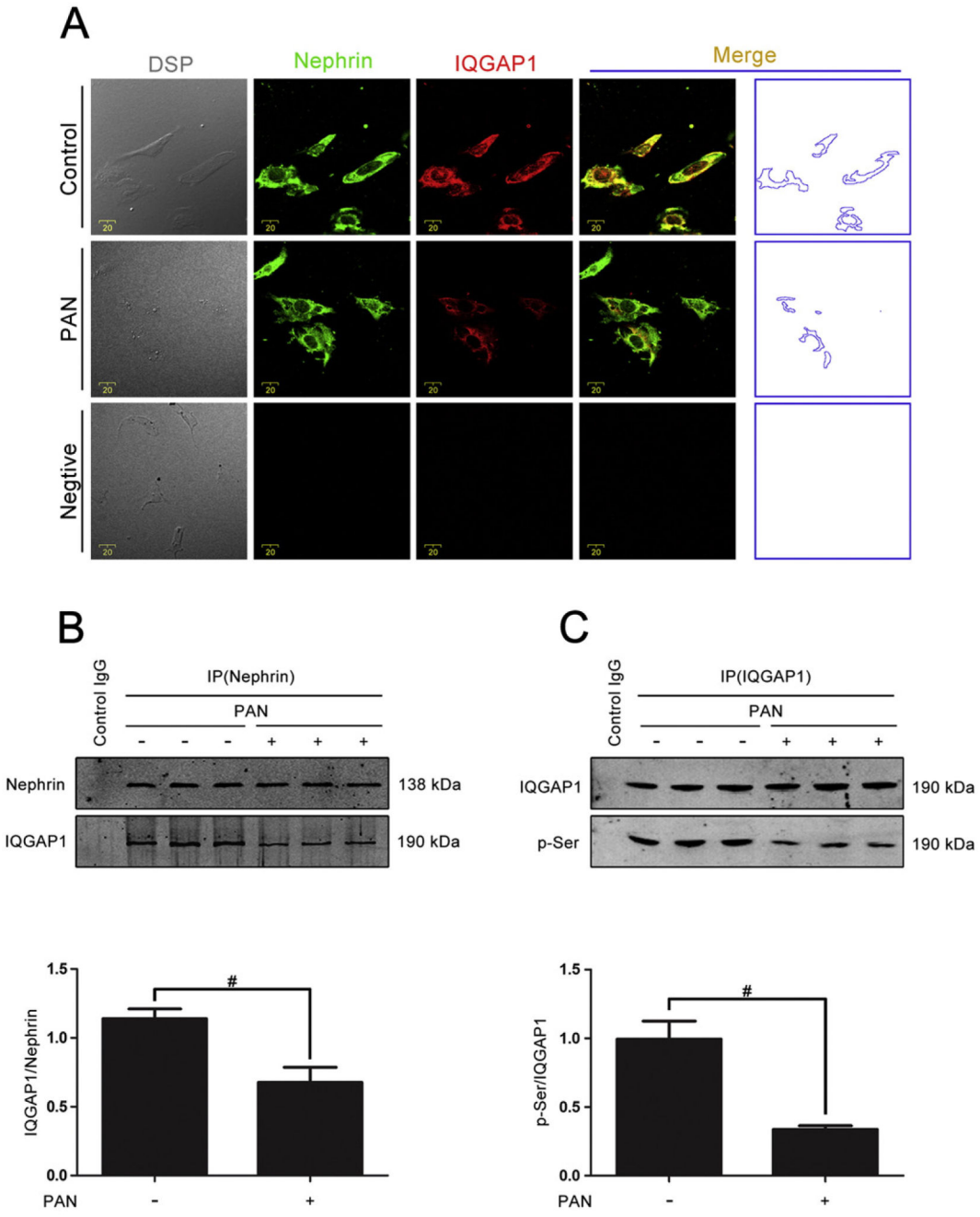

Fig. 3.

The interaction between IQGAP1 and nephrin and the phosphorylation of IQGAP1 in PAN-stimulated podocytes. (A) Double-immunolabeling of nephrin and IQGAP1 in cultured podocytes (original magnification ×400). The area indicated by the blue dotted line is the region of colocalized nephrin and IQGAP1. Scale bar = 20 μm. (B) Co-immunoprecipitation analysis between IQGAP1 and nephrin in podocytes treated with PAN (50 μg mL^{-1} for 6 h) (n = 3). Control IgG is a normal rabbit IgG that replaced the anti-nephrin pAb in the precipitation process. (C) The phosphorylation of IQGAP1 detected by co-

immunoprecipitation ($n = 3$). Control IgG is a normal rabbit IgG that replaced the anti-IQGAP1 pAb in the precipitation process. #$p < 0.01$ relative to control.

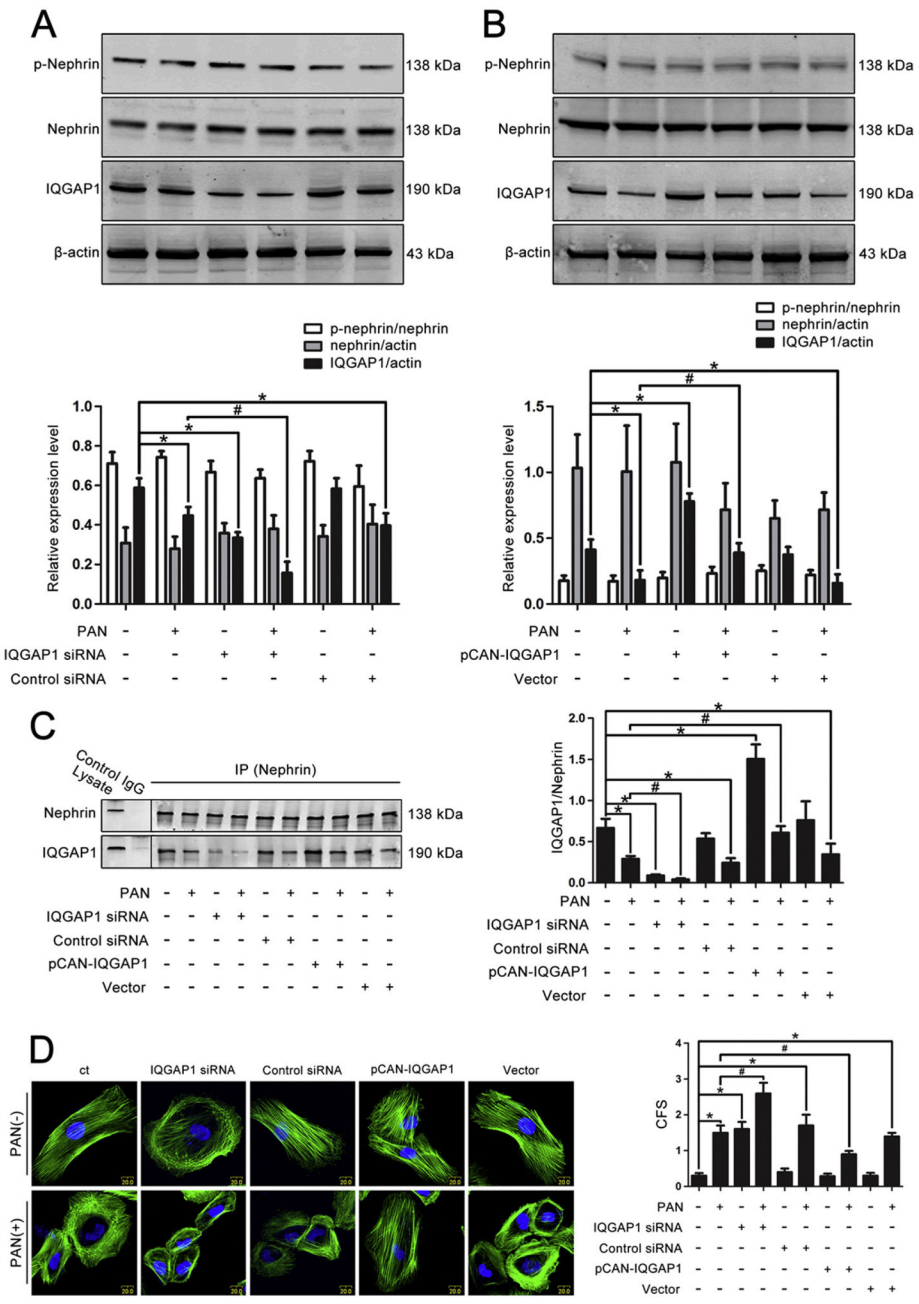

Fig. 4.

Effects of altered IQGAP1 expression on nephrin, phosphorylated nephrin, cytoskeletal reorganization, and the interaction between IQGAP1 and nephrin in podocytes. (A) Western blotting analysis of the expression of nephrin, phosphorylated nephrin and IQGAP1 in cultured podocytes stimulated by PAN and pre-transfected with IQGAP1 siRNA or scrambled siRNA (n = 3). (B) Western blotting analysis of the expression of nephrin, phosphorylated nephrin and IQGAP1 in cultured podocytes stimulated by PAN and pre-transfected with the wild-type IQGAP1 plasmid or null vector (n = 3). (C) Co-immunoprecipitation analysis between IQGAP1 and nephrin in podocytes transfected with

the relevant siRNA or plasmid in the presence or not in the presence of PAN ($n = 3$). Lysate indicates the podocyte lysate and was used as a positive control. Control IgG is a normal rabbit IgG and was used as a negative control. (D) FITC-phalloidin staining of the actin cytoskeleton in podocytes with altered IQGAP1 expression in the presence or not in the presence of PAN (original magnification ×400), and the quantitative analysis of CFS ($n = 100$). The nuclei were stained with DAPI. Scale bar = 20 μm. *$p < 0.05$ relative to control, #$p < 0.05$ relative to PAN-treated cells.

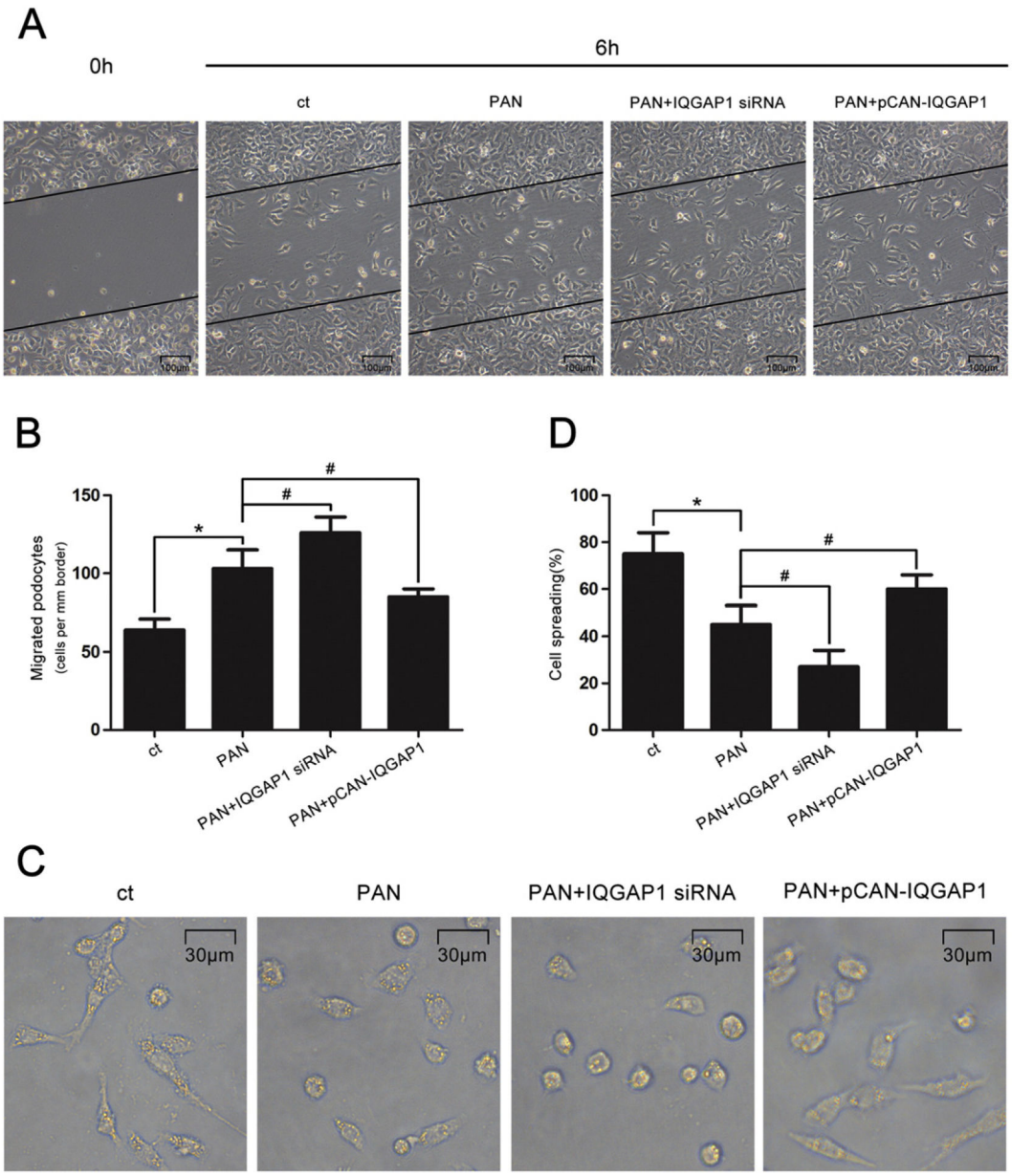

Fig. 5.

Involvement of IQGAP1 in podocyte migration and spreading. (A) Representative migration results of podocytes stimulated with PAN and pre-transfected with IQGAP1 siRNA or plasmids (original magnification ×100). Scale bar = 100 μm. (B) Quantitative analysis of podocyte migration. ($n = 3$). (C) Representative spreading images of podocytes stimulated with PAN in the presence of IQGAP1 siRNA or plasmids (original magnification ×400). Scale bar = 30 μm. (D) Quantitative analysis of podocyte spreading ($n = 3$). *$p < 0.05$ relative to control, $^{\#}p < 0.05$ relative to PAN-treated cells.

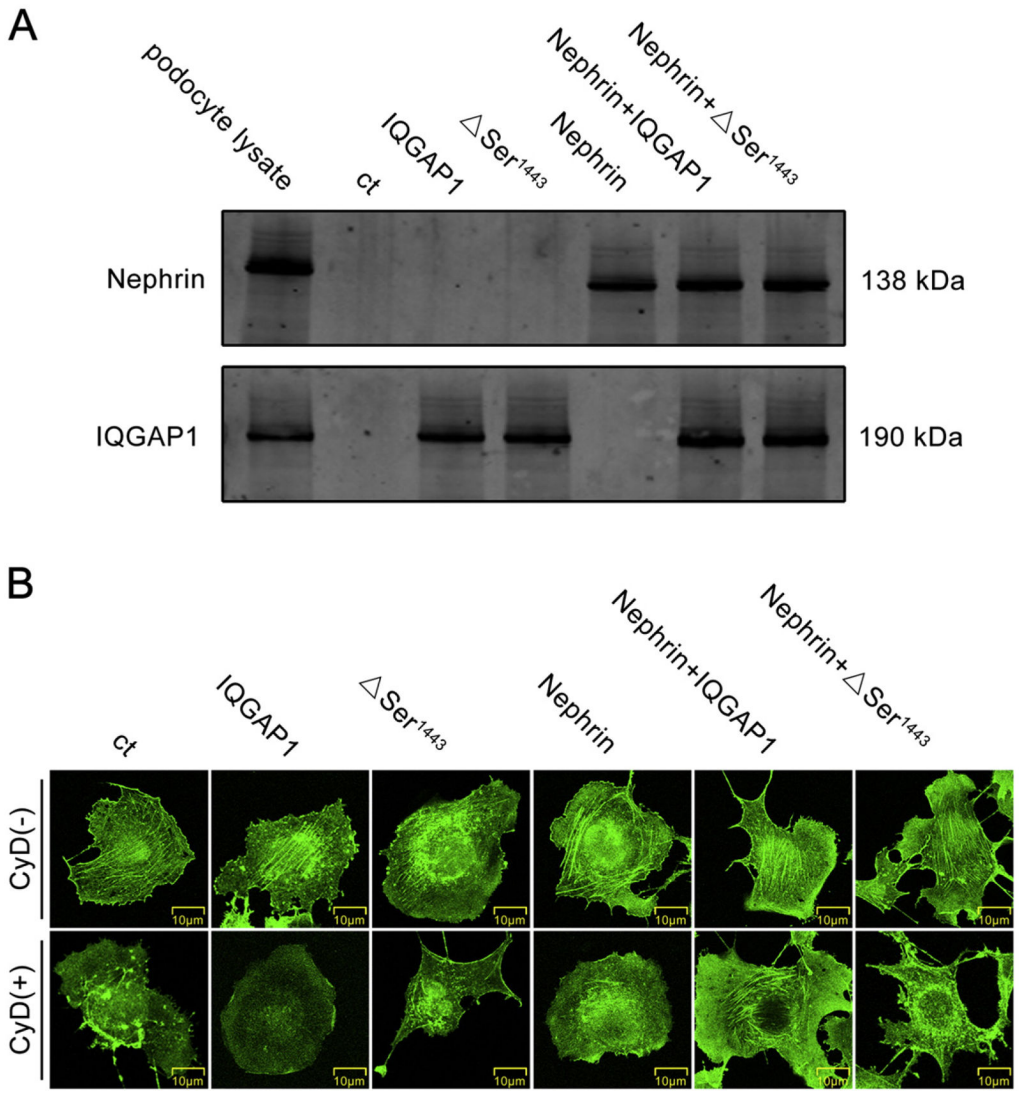

Fig. 6.

Involvement of the nephrin–IQGAP1 interaction and IQGAP1 phosphorylation in cytoskeletal regulation. (A) Western blotting analysis of the expression of nephrin and IQGAP1 in COS7 cells transfected with wild-type IQGAP1, mutated IQGAP1 (ΔSer1443) or wild-type nephrin plasmids. The podocyte lysate was used as a positive control. (B) The FITC-phalloidin staining of actin cytoskeleton in COS7 (or NCOS7) cells pretreated with CyD and transfected with IQGAP1 wild-type or mutated plasmids (original magnification ×400). Scale bar = 10 μm.

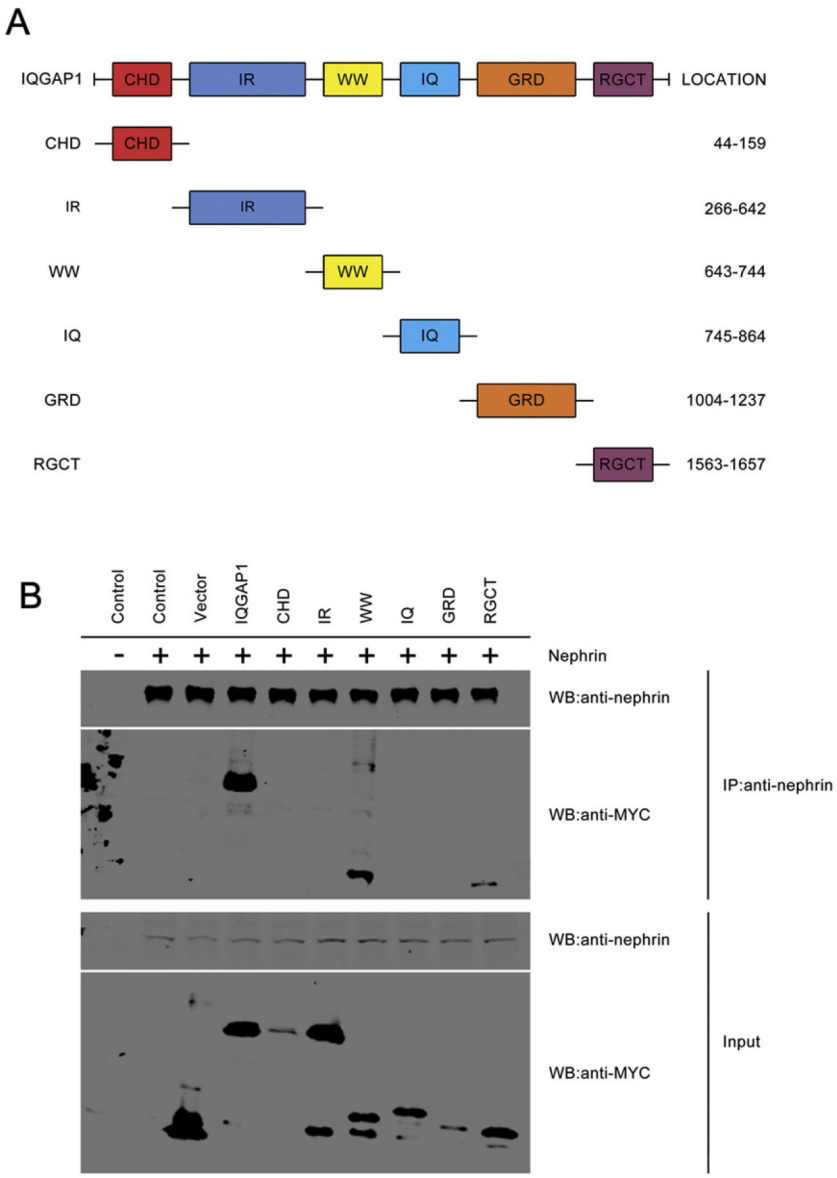

Fig. 7.

Identification of the specific domains of IQGAP1 necessary for interacting with nephrin. (A) Schematic diagram depicting the domain organization of human IQGAP1 and various truncated IQGAP1 mutants. The location indicates the amino acid residues. (B) Detection of the nephrin binding sites in IQGAP1. The co-immunoprecipitation study was performed using COS7 cell lysates with (+) or without (−) nephrin overexpression and each derivative molecule of IQGAP1. Input: total protein extract.

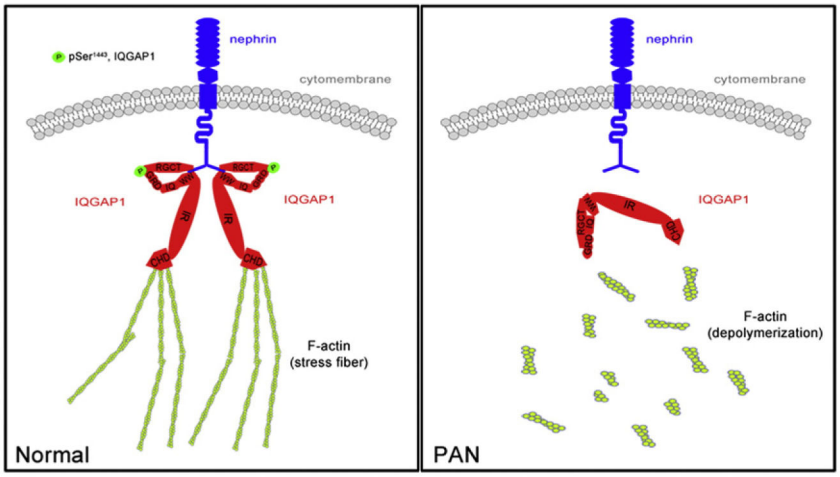

Fig. 8.

A schematic model for the involvement of IQGAP1 in actin cytoskeleton organization in podocytes.

Table 1

Detailed IQGAP1 plasmid information.

Plasmids	Amino acids	Primers
Δ1443(S → A)	1443	Sense: 5′-ATGAAAAAGTCAAAA**G**CTGTAAAGGAAG-3′ Anti-sense: 5′-**C**TTTTGACTTTTTCATCTTGTCAGG-3′
CHD	44–159	Sense: 5′-CCGCTCGAGCTCTTTGTCATTTGGAAGAAGC-3′ Anti-sense: 5′-CGGGGTACCTTACAGGTACAAACTGAGTGCATG-3′
IR	266–642	Sense: 5′-CCGCTCGAGCTAAGCAGGACAAAATGACAAATGC-3′ Anti-sense: 5′-CGGGGTACCTTATGTTTTGCCAACATCACCACTTTC-3′
WW	643–744	Sense: 5′-CCGCTCGAGCTCTGAGTGCCCTTCGCTCC-3′ Anti-sense: 5′-CGGGGTACCTTAGGCCAGCCACAGCTGTTC-3′
IQ	745–864	Sense: 5′-CCGCTCGAGCTAATGAAGGCCTGATCACCAGG-3′ Anti-sense: 5′-CGGGGTACCTTAAGGATCCTCAGCATTGATGAGAG-3′
GRD	1004–1237	Sense: 5′-CCGCTCGAGCTTCTGTAATCTTCACACTCTACAAC-3′ Anti-sense: 5′-CGGGGTACCTTAGGAAGCAGCATGCTGAAG-3′
RGCT	1563–1657	Sense: 5′-CCGCTCGAGCTTATACAGCAGCAAGACTACATG-3′ Anti-sense: 5′-CGGGGTACCTTACTTCCCGTAGAACTTTTTGTTGAG-3′